Role and Mechanisms of Probiotics in Regulating the ROS/JNK Signaling Pathway in the Pathogenesis of Nonalcoholic Fatty Liver Disease.

HuiYuan Xu
The Affiliated Hospital of Southwest Medical University https://orcid.org/0000-0002-7795-0480
LeiLei Yang
The Affiliated Hospital of Southwest Medical University
YuMei Huang
The Affiliated Hospital of Southwest Medical University
ChangPing Li (lichangping1965@sina.com)
The Affiliated Hospital of Southwest Medical University

Research

Keywords: Nonalcoholic fatty liver disease, methionine- and choline-deficient diet, probiotics, ROS/JNK signaling pathway, apoptosis

DOI: https://doi.org/10.21203/rs.3.rs-164978/v1

Abstract

This study was aimed to investigate the impact of probiotics on regulating the ROS/JNK signaling pathway their underlying mechanism of action in the treatment of nonalcoholic fatty liver disease. For this purpose, male C57BL/6 mice were randomly divided into three groups: control, probiotics, and model groups. Methionine and choline deficiency (MCD) diets were fed for four weeks to establish a NAFLD mouse model. Serum levels of ALT, AST, TC, and TG were detected. Moreover, the pathological changes of the liver and ileum tissues were observed by hematoxylin and eosin (H&E) staining, and the content of reactive oxygen species (ROS) in liver tissues was determined. In addition, the levels of D-lactic acid and plasma and small intestine diamine oxidase were measured to evaluate the effects of probiotics on the intestinal tract of NAFLD mice. The expression levels of p-JNK, Bax, and Caspase-3 were established to analyze the regulatory mechanism of probiotics on the JNK signaling pathway. We found that probiotics improve liver function, repair intestinal barrier and significantly suppressed oxidative stress, JNK phosphorylation. Moreover, the application of probiotics regulated the expression of signaling pathway-related proteins and promoted the intestinal barrier function repair and decreased intestinal permeability. The data above suggest that probiotics alleviate NAFLD, whose mechanism might be associated with the regulation of ROS/JNK signaling pathway and the suppression of oxidative stress and apoptosis.

Introduction

Nonalcoholic fatty liver disease (NAFLD) is the most frequent chronic progressive liver disease all over the world, with a global incidence of approximately 25% (1, 2). It is a complex disease whose pathogenesis remains unclear. An earlier study showed that NAFLD is closely associated with metabolic abnormalities, oxidative stress, inflammatory response, apoptosis, and other factors (3). To date, clinical guidelines indicate that dietary interventions and lifestyle changes are the major factors involved in the treatment of NAFLD and its complications while no specific drugs are available for NAFLD therapy (4). Therefore, it is critically important to investigate and discover novel therapeutic targets and approaches.

C-Jun N-terminal kinase (JNK) is one of the most important pathways in the mitogen-activated protein kinase (MAPK) family that is mainly involved in stress response and apoptosis, among other physiological processes (5). The accumulation of reactive oxygen species (ROS) induces apoptotic signal transduction and activates apoptotic proteins, such as caspase-3 and Bax, causing apoptosis (6, 7). The bodily production of ROS is induced through the action of various factors causing oxidative stress, leading to activation of apoptosis signal-regulating kinase 1 (ASK1). In turn, JNK phosphorylation is promoted, and phosphorylated JNK further activate and promote the overexpression of the apoptosis proteins Bax, cysteinyl aspartate-specific proteinase-3 (caspase-3), resulting in liver cell apoptosis, which can lead to liver degeneration and necrosis (Fig. 1) (6, 8, 9).

Probiotics are a group of bioactive microorganisms that are beneficial to the host and improve its microecological balance and a favorable impact on the status and function of the intestinal tract (10, 11). Probiotics may improve the intestinal epithelial barrier function and reduce intestinal permeability,

inflammation, and oxidative stress by regulating the abundance and diversity of the natural intestinal flora; thus, it can be applied in the treatment of NAFLD, but their specific mechanism of action has not yet been clarified (12). Moreover, the efficacy of probiotics in metabolic disease treatment remains controversial, and further studies are needed to assess their safety and significance in that respect. Hence, the purpose of this investigation was to elucidate the role and mechanism of probiotics in regulating ROS/JNK signaling pathway in the treatment of NAFLD, which would provide novel insights, further evidence, and reference for the clinical use of probiotics in the treatment of NAFLD.

Materials And Methods

Lactobacillus plantarum N3117 isolation and culture methods

Lactobacillus plantarum N3117 was isolated from Inner Mongolia traditional fermented milk and stored in the central laboratory of Affiliated Hospital of Southwest Medical University,was cultured at 37℃ for 24 h in de Man, Rogosa, and Sharpe (MRS) broth.Bacteria were collected from MRS broth cultures by centrifugation (6000g for 10 min at 4℃).Afterwards, phosphate buffered saline (PBS) was used to wash the particles twice and live bacteria used as oral probiotic supplements were suspended in sterile saline.Each bacterial suspension was given an adjusted oral dose of 1.0 x 108 colony-forming units (CFU)/ day/mouse.

Mice and materials

Male C57BL/6 mice were purchased from the Experimental Animal Research Center of Hubei. (six weeks, n = 18, 20–25 g). All animals received care according to the guidelines of the Institutional Animal Care and Use Committee of Southwest Medical University (Luzhou, China), and the experiment had been approved by the Experimental Animal Ethics Committee of Southwest Medical University (Approval no 2020439). Methionine- and choline-deficient (MCD) and methionine- and choline-sufficient (MCS) diets were purchased from Nantong Troffin Technology Co. Ltd. Alanine aminotransferase (ALT),aspartate aminotransferase (AST), total cholesterol (TC), triglyceride (TG), D-lactic acid (D -Lac), reactive oxide species (ROS,) and diamine oxidase (DAO) assay kits were purchased from Nanjing Jian Cheng Bioengineering Institute (Nanjing, Jiangsu, China).

NAFLD model

All C57BL/6 mice were fed normal diet and water ad libitum for a week at room temperature of 18°C–22°C, humidity of 50%, and day-night cycle of 12 h. After another week of new environment acclimation, C57BL/6 mice (n = 18) were randomly divided into three groups (n = 6 in each group): control, probiotic, and model group. In the model and probiotic groups, mice were fed MCD diet, whereas in the control group, MCS diet was applied for four weeks(The duration of probiotics treatment was determined by preliminary studies). Then, a mouse was randomly selected from each group and killed by Cervical dislocation. H&E staining of the liver tissue was used to confirm the successful establishment of the

model. In the probiotic group, mice received probiotics gavage once a day, whereas the control and the model groups were given the same amount of saline gavage once a day for four weeks. After the drug intervention was complete, the mice were fasted for 12 h, and their weight was measured. Next, using pentobarbital sodium for intraperitoneal injection anesthesia, blood was collected from the heart, followed by settlement for 1 h and centrifugation for 10 min at 2000 g. After centrifugation, we collected the supernatant and preserved it at -80°C for analyses of the levels of lipids, transaminases, and related parameters. Liver and ileum tissues were dissected and weighed. Then, part of them was fixed in 4% formaldehyde and sent to the Pathology Department for H&E staining and immunohistochemical analysis. The remaining liver and ileum tissues were frozen at -80°C in a refrigerator for further Western blot and PCR analyses.

Biochemical analysis

After the mice were killed, blood samples were taken from the heart. Then, the blood samples were centrifuged at 5000 rpm for 20 min for supernatant serum extraction. The levels of ALT, AST, TG, TC, D-Lac, DAO, and ROS were determined by ALT, AST, TG, TC, D-Lac, DAO, and ROS assay kits (Nanjing Jiancheng Bioengineering Institute, Nanjing, Jiangsu, China).

Histopathology

Liver and ileum tissues were collected after the mice were killed, and H&E staining was used to observe their pathological changes. The intestinal tissue injury was evaluated by Chiu's score (13)using the following scale of 0–5 points: 0, normal intestinal mucosal villi; 1, Gruenhagen's space generally at the apex of the villus; 2, elevation of the intestinal mucosal epithelium from the intrinsic membrane and expansion of the subepithelial space; 3, a mass of epithelial lifting down the sides of villi; 4, denuded villi of lamina propria and telangiectasia exposed; and 5,disintegration of the lamina propria, bleeding, and anabrosis.The liver tissue was assessed by NAFLD activity score (NAS) (14).The NAS (0–8 points) was assessed by i) hepatocyte steatosis: 0 points (< 5%);1 point, 5–33%);2 points, 34–66%;3 points > 66%;ii) inflammation in the hepatic lobule (count necrotic foci at x20 magnifica tion): 0 points, none;1 point, < 2;2 points, 2–4;3 points, > 4;and iii) hepatocyte ballooning: 0 points, none;1 point, rare;2 points, many.NASH was excluded if the NAS was < 3, and NASH was diagnosed if the NAS was > 4.

Western blot

Liver and ileum tissues were cleaned with precooled PBS buffer 2–3 times to purify the blood. Next, the appropriate volume of total cell protein extraction reagent was placed into an ice bath (protease inhibitor was added a few minutes before use), where the homogenate was hatched lasted for 30 min. The homogenate was centrifuged at 4°C and 13,000 g for 5 min, followed by supernatant collection. Further, the concentration of the supernatant protein was measured by a BCA protein concentration assay kit (Wuhan Aspen Biotechnology Co., Ltd., Wuhan, China). The right quantity of protein loading buffer was added to the protein samples, and they were boiled in a water bath at 95°C–100°C for 5 min and transferred onto PVDF membranes (Millipore Co., Ltd., Shanghai, China). Next, the confining solution was removed, and the primary antibody was added (Table I) and left undisturbed overnight at 4°C. The

secondary antibody (Table II) was then added, followed by incubation at room temperature for 30 min. The fresh ECL mixture was next added to the protein side of the membrane for its exposition in the in the dark.

Real-time quantitative PCR

Total mRNA was extracted from the liver employing a TRIpure RNA Extraction Reagent kit (ELK Biotechnology Co., Ltd., Wuhan, China). The first-strand of cDNA of Bax and Caspase-3 were synthesized by the EntiLink 1st Strand cDNA Synthesis Kit (ELK Biotechnology, Co., Ltd., Wuhan, China).The primers sequences were shown in Table III. The real-time quantitative fluorescence PCR was completed on a StepOne real-time PCR instrument of Life Technologies, and each sample was detected by employing the EnTurbo SYBR Green PCR SuperMix kit (ELK Biotechnology, Co., Ltd., Wuhan, China).The relative quantitative of gene expression was evaluated by the 2-ΔΔCt method (15).

Immunohistochemistry

The liver tissues were removed from the mice and fixed with 10% formaldehyde and embedded with paraffin, and sectioned. Sections were incubated with primary antibody (Table IV) and the secondary antibody (Table V), and DAB solution (Zhongshang Jinqiao Biotechnology Co., Ltd., Beijing, China) was added to color.

Statistical analysis

SPSS 25.0 was used for all statistical analyses. The data were expressed as means ± SD for each group. One-way analysis of variance (ANOVA) was among the groups. A value of $P < 0.05$ was considered to indicate statistically significant differences.

Results

Effects of probiotics on liver function and lipid levels in serum

Serum ALT, AST, TC, and TG levels in the model group were considerably higher than those in the control group(Fig. 1). However, four-week probiotics administration lowered the serum levels of ALT, AST, TC, and TG.

Effect of probiotics on hepatic pathology

In the control group, H&E staining results showed orderly arrangement of hepatocytes, with no fat droplet deposition and inflammatory cells; the hepatic lobules had a normal structure (Fig. 2a and A). Nevertheless, the structure of the hepatic lobule was disordered and the arrangement of hepatocytes was unclear boundaries. Besides, there were more fat droplets and inflammatory cells in the cytoplasm in the model group (Fig. 2c and C). Four-week probiotics treatment alleviated all these signs (Fig. 2b and B).

Effect of probiotics on the intestinal barrier function and permeability

Serum D-Lac levels of and the serum and ileum levels of DAO were known to be important indicators for measurements of intestinal barrier function and permeability. In our study, the levels of D-Lac and DAO in the model group were significantly higher than those in the control group. However, the serum levels of D-Lac and DAO in the probiotics-treated group were lower than those in the model group. Moreover, the ileum level of DAO in the model group was significantly higher than that in the control group, but the treatment with probiotics considerably decreased this level, suggesting that probiotics could repair the intestinal barrier and reduce intestinal permeability (Fig. 3).

The pathological results in our investigation showed that the ileum mucosa in the control group was intact, and the intestinal villi were complete and neatly arranged, without any infiltration of inflammatory cells. However, in the model group the ileum mucosal structure was seriously damaged, with loose and disorderly villi arrangement. Importantly, the ileum mucosa in the probiotic group had fewer injuries and the villi were arranged more neatly (Fig. 4). Besides, the ileum tissue of the control group had the lowest Chiu's score range (0–1), whereas that of the model group was 3–4, and the one of the probiotic group was 1–2 (Fig. 5).

The tight junction protein ZO-1 was critically involved in intestinal barrier function maintenance and had been considered the most reliable marker protein for tight junction detection. Western blot results revealed obviously lower expression of ZO-1 in the model than in the control group. However, the expression of the intestinal tight junction protein ZO-1 was upregulated in the probiotic group in contrast to the model group (Fig. 6A,E).

Effect of probiotics on ROS/JNK signaling pathway in NAFLD

To verify the regulation effect of probiotics on the ROS/JNK signaling pathway in NAFLD mice, we detected the expression of ROS/JNK signaling pathway-associated proteins in the liver. The consequences demonstrated that ROS was observably added in the model group; moreover, it was decreased after four weeks of probiotics treatment (Fig. 7). Subsequently, we used Western blot analysis to explore the JNK signaling pathway mechanisms of the probiotics action in the treatment of NAFLD. We established a dramatically higher increase in the p-JNK, Bax, and Caspase-3 levels in the model group than in the control group, whereas probiotics obviously suppressed the expression of p-JNK, Bax, and Caspase-3 in the probiotics group (Fig. 6B–E). These results were also confirmed by immunohistochemical staining (Fig. 9). qPCR assays showed that probiotics suppressed apoptosis by inhibiting the expression of the related genes in the JNK signaling pathway (Fig. 8). These results indicated that the oxidative stress induced by ROS in MCD-induced NAFLD can cause apoptosis, but probiotics can effectively attenuate this liver injury.

Discussion

NAFLD is currently the most frequently occurring of all chronic liver diseases, with a yearly rise in morbidity and mortality (1). Despite the abundance of national and foreign studies and the deepened understanding on NAFLD, its pathogenesis is still unclear, and the treatment options are very limited (1, 2). Thus, at this stage, the establishment of animal models is still necessary in the research on NAFLD pathogenesis and the discovery of potential novel therapeutic targets. Various approaches have now been used for the establishment of animal NAFLD models, which can be divided into two major categories; the first method is based on the establishment of animal NAFLD models through diet induction; the second is realized by specific gene knockout through genetic modification (16–19).

The animal model of diet induction has been often used at home and abroad, which can simulate the natural formation process of human NAFLD, with a high success rate, low mortality rate, and good repeatability (20–24). The most commonly applied diet models are choline-deficient, L-amino acid-defined (CDAA) diet, high-cholesterol diet (HCD), MCD, high-sugar diet, etc. Unlike other diet models, MCD can lead to insulin resistance and a significant weight loss, which is inconsistent with the human metabolic model. However, MCD diet can well simulate the pathological characteristics of NASH, and the time for its implementation is short (approximately 2–4 weeks). Therefore, MCD diet has been most extensively investigated and applied in the development of NAFLD models (20–24). Therefore, our mouse NAFLD model was developed using an MCD diet, which was simple and rapid. We assumed that the establishment of this model was closer to the natural course of the disease in patients with NAFLD. Here, we successfully set up a NAFLD mice model and found that a four-week probiotics treatment reduced the liver function damage caused by MCD diet and attenuated liver and intestinal pathological injuries.

The gut and the liver are closely linked by their tight anatomical and functional relationships, also collectively known as the “gut–liver axis” (25, 26). Accumulating recent evidence from many human and animal model studies has shown that gut microbiota dysfunction is conducive to the development and progression of NAFLD (27). The increase in intestinal permeability was found to cause injuries in the intestinal mucosal barrier, leading to the overproduction of bacteria in the intestinal cavity, destruction of the intestinal microenvironment, and the production of a large number of toxic metabolites and endotoxins (26). On the one hand, the endotoxins entering the blood circulation not only directly damage the intestinal mucosal epithelial cells, but also induce intestinal microvasculature contractions and intestinal tissue ischemia and hypoxia, leading to excessive ROS production. Meanwhile, the increase in the intestinal permeability augments endotoxin absorption, which is also a huge burden on the liver (28, 29). On the other hand, because of the presence of the intestine-liver axis, the endotoxins entering the blood circulation also act directly on the liver, causing its inflammation by activating Toll-like receptors (29–31).

A recent clinical trial found that probiotics alleviated intestinal microecological and metabolic disorders in patients with NAFLD (32). ALT and AST concentrations are considered important markers for liver injury evaluation. Our results showed significantly increased serum AST and ALT levels in the model group and

pathologically damaged liver tissue. After four weeks of probiotics treatment, the elevated serum ALT, AST, TC, and TG levels, induced by the MCD diet, were alleviated and liver steatosis improved, demonstrating the beneficial effects of probiotics on the liver.

Lipid peroxidation and oxidative stress are vital pathogenetic mechanisms of NAFLD, and thus their suppression may serve as an effective method for NAFLD prevention or intervention (33). Studies have shown that excessive free fatty acids (FFAS) in the liver cells induce lipid peroxidation during NAFLD, which considerably increases the production of ROS (33, 34). On the one hand, the produced ROS promote the release of TNF-α, which triggers inflammation through the NF-κB signaling pathways and aggravates the inflammatory response of the liver. On the other hand, ROS can participate in the JNK signaling pathway as the second messenger, eventually activating the JNK signaling pathway and inducing hepatocyte apoptosis (34, 35). To elucidate the potential mechanism of probiotics action in NAFLD remedy, we analyzed the expression of ROS/JNK signaling pathway-related factors.

JNK is well recognized as an important signaling involved in stress response and apoptosis, which is activated by oxidative stress, DNA damage and UV exposure, and subsequently regulates the downstream targets expression, such as that of Bax and Caspase-3 (35, 36). Bax is a pro-apoptotic gene, and Caspase-3 is critically involved in apoptosis (37). In this study, we established that probiotics exerted an important part in antioxidant stress and apoptosis alleviation. The large amount of ROS, produced due to action of different stimuli, activates the JNK pathway through a JNK-specific kinase, JNKK. Then, JNK phosphorylation enhances the activity of the transcription factor complex AP-1, resulting in upregulated expression of pro-apoptotic proteins, such as p53, Bax, and TNF, but inhibited expression of apoptotic proteins such as Bcl-2. Subsequently, the overexpressed pro-apoptotic proteins apply to and accelerate the release of cytochrome C from the mitochondria into cytoplasm. Next, cytochrome C binds to caspase-9, and that complex then interacts with caspase-3. Finally, activated caspase-3 binds to apoptotic substrates and causes apoptosis (37–39). In a previous study, the inhibition of JNK phosphorylation reduced liver fat deposition and improved liver function and inflammatory response in animals with MCD-induced NAFLD (40). To further confirm the anti-inflammatory effect of probiotics on MCD-induced oxidant stress and apoptosis, we investigated the changes in JNK downstream signaling. Our results showed that the expression levels of ROS, P-JNK, Bax, and caspase-3 were significantly increased in the model group; the oxidative stress response was enhanced and liver cell apoptosis increased. Moreover, we found that probiotics diminished ROS production, inhibited JNK phosphorylation, significantly suppressed the expression of Bax and Caspase-3 in the downstream JNK signaling pathway, and further impeded cell apoptosis, which alleviated NAFLD. These results indicate that probiotics can be utilized as a therapeutic target for the treatment of NAFLD by regulating the ROS/JNK signaling pathway. This study provides a potential target for NAFLD and additional evidence for the significance of the clinical use of probiotics in the treatment of NAFLD.

However, this study has some limitations. First of all, it was focused on the expression of pro-apoptotic genes in the JNK signaling pathway, but did not examine the importance of the expression of anti-apoptotic genes and related proteins. Second, the test results of a single sex of mice and a single NAFLD

modeling method may be controversial to some extent, and this study needs to be supplemented and verified in the later stage by combining different genders of mice and different NAFLD modeling methods.Finally, we only analyzed the intestinal barrier function and permeability, but did not analyze and evaluate the changes of gut microbiota in mice. If the above limitations had been overcome, our experimental results would have been more reliable. Multiple mechanisms of probiotics action can be exerted in the treatment of NAFLD, but only one of them was investigated in this study. Therefore, future studies should be performed for further clarification of the potential mechanisms of probiotics action in the treatment of NAFLD.

Declarations

Acknowledgements

Not applicable.

Funding

No funding was received.

Availability of data and materials

All data employed or analyzed during this study are available upon request from the author.

Authors' contributions

HYX and CPL participated in the design and review of the article. HYX and LLY wrote and revised the manuscript. HYX, LLY, and YMH were responsible for the procurement of experimental reagents and testing of various indicators. HYX, LLY, and YMH conducted data collection and statistical analyses. All authors approved the final version of the manuscript.

Ethics approval and consent to participate

The ethical review and approval of the animal experiments was performed by the Ethics Committee of Affiliated Hospital of The Southwest Medical University (Luzhou; Approval no. 2020439).

Patient consent for publication

Not applicable.

Competing interests

The authors declare that they have no competing interests.

References

1. Xing-Tong S,Huai-Yuan G,Jin-Jin X,Jinliang W.Inhibition of lncRNA HULC improves hepatic fibrosis and hepatocyte apoptosis by inhibiting the MAPK signaling pathway in rats with nonalcoholic fatty liver disease.*J Cell Physiol.*234:18169-18179(2019).
2. Becky Ching-Yeung Y,Deborah K,Vincent Wai-Sun W..Magnitude of Nonalcoholic Fatty Liver Disease: Eastern Perspective.*J Clin Exp Hepatol*.9:491-496(2019).
3. Simona M,et al. Pathophysiological, Molecular and Therapeutic Issues of Nonalcoholic Fatty Liver Disease: An Overview.*Int J Mol Sci*.20:1948(2019).
4. Zobair M Younossi,Aaron B Koenig,Dinan Abdelatif,Yousef Fazel,Linda Henry,Mark Wymer.Global epidemiology of non-alcoholic fatty liver disease-meta-analytic assessment of prevalence,incidence and outcomes. *Hepatology.*64:73-84(2016).
5. Qianwen C,et al.N-n-Butyl Haloperidol Iodide Ameliorates Oxidative Stress in Mitochondria Induced by Hypoxia/Reoxygenation through the Mitochondrial c-Jun N-Terminal Kinase/Sab/Src/Reactive Oxygen Species Pathway in H9c2 Cells.*Oxid Med Cell Longev*.7417561(2019).
6. Yukai X,et al.Brusatol inhibits growth and induces apoptosis in pancreatic cancer cells via JNK/p38 MAPK/NF-κb/Stat3/Bcl-2 signaling pathway.*Biochem Biophys Res Commun.* 487:820-826(2017).
7. Yang Q,Qian L,Zhang S.Ginsenoside Rh1 Alleviates HK-2 Apoptosis by Inhibiting ROS and the JNK/p53 Pathways.*Evid Based Complement Alternat Med.*3401067(2020).
8. Zhuang J,et al.BDE-47 induced apoptosis in zebrafish embryos through mitochondrial ROS-mediated JNK signaling.*Chemosphere.*258:127385(2020).
9. Lei H,et al.Epigenetic modulation of the MAPK pathway prevents isoflurane-induced neuronal apoptosis and cognitive decline in aged rats.*Exp Ther Med.*20:35(2020).
10. Wieland A,Frank DN,Harnke B,Bambha K.Systematic review: microbial dysbiosis and nonalcoholic fatty liver disease.*Aliment Pharmacol Ther*.42:1051-63(2015).
11. Xue L,et al.Probiotics may delay the progression of nonalcoholic fatty liver disease by restoring the gut microbiota structure and improving intestinal endotoxemia.*Sci Rep.* 7:45176(2017).
12. Wang W,et al.Lactobacillus paracasei Jlus66 extenuate oxidative stress and inflammation via regulation of intestinal flora in rats with non alcoholic fatty liver disease.*Food Sci Nutr.*7:2636-2646(2019).
13. Yasemin Dere G,Özlem Boybeyi T,Pınar A,Üçler K,Mustafa Kemal A..The effects of ozone on the acute phase of intestinal ischemia-reperfusion injury in rats.*Ulus Travma Acil Cerrahi Derg*.26:651-656(2020).
14. Mahamid M, et al. Folate and B12 levels correlate with histological severity in NASH patients. *Nutrients.*10:440(2018).
15. Yile F,et al. Improvement and Application of qPCR (Real-Time Quantitative Polymerase Chain Reaction) Data Processing Method for Home-Made Integrated Nucleic Acid Detection System.*Nanosci Nanotechnol*.20:7369-7375(2020).

16. Van Sinderen M L, et al.Hepatic Glucose intolerance precedes hepaticsteatosis in the male aromatase knockout (ArKO) mouse.*PLoS One.*9:e87230(2014).
17. Kroh A,et al.Mouse Models of Nonalcoholic Steatohepatitis: Head-to-Head Comparison of Dietary Models and Impact on Inflammation and Animal Welfare.*Gastroenterol Res Pract.*7347068(2020).
18. Ching Lau JK,,Xiang Z,Jun Y.Animal models of non alcoholic fatty liver disease: Current perspectives and recent advances.*J Pathol.*241:36-44(2017).
19. Van Herck MA, Vonghia L and Francque SM. Animal models of nonalcoholic fatty liver disease a starter's guide. *Nutrients.* 241:36-44(2017).
20. Fisher Wellman KH,et,al.A direct comparison of metabolic responses to high fat diet in C57BL/6J and C57BL/6NJ mice.*Diabetes.* 65:3249-3261(2016).
21. Mei-Ying L,Guan-Ping F,Hong W,Rui-Li Y,Zhenlin X,Yuan-Ming S.Deacetylated konjac glucomannan is less effective in reducing dietary induced hyperlipidemia and hepatic steatosis in C57BL/6 mice. *J Agric Food Chem*. 65:1556-1565(2017).
22. Ghosh SS, Wang J, Yannie PJ, Sandhu YK,Korzun WJ,Shobha G.Dietary Supplementation with Galactooligosaccharides Attenuates High-Fat, High-Cholesterol Diet-Induced Glucose Intolerance and Disruption of Colonic Mucin Layer in C57BL/6 Mice and Reduces Atherosclerosis in Ldlr-/- Mice. *J Nutr.* 150:285-293(2020).
23. Lau JK, Zhang X and Yu J. Animal models of non alcoholic fatty liver disease: Current perspectives and recent advances. *J Pathol.* 241:36-44(2017).
24. Van Herck MA, Vonghia L and Francque SM.Animal models of nonalcoholic fatty liver disease a starter's guide. *Nutrients.* 9:1072(2017).
25. Mu J,Tan F,Zhou X,Xin Z.Lactobacillus fermentum CQPC06 in naturally fermented pickles prevents non-alcoholic fatty liver disease by stabilizing the gut–liver axis in mice.*Food Funct*.11:8707-8723(2020).
26. Di Ciaula A,et,al.Liver Steatosis, Gut-Liver Axis, Microbiome and Environmental Factors. A Never-Ending Bidirectional Cross-Talk.*J Clin Med.* 9:2648(2020).
27. Mungamuri SK,Vijayasarathy K.Role of the Gut Microbiome in Nonalcoholic Fatty Liver Disease Progression.*Crit Rev Oncog.* 25:57-70(2020).
28. Khan I,et,al.Alteration of Gut Microbiota in Inflflammatory Bowel Disease (IBD): Cause or Consequence? IBD Treatment Targeting the Gut Microbiome.*Pathogens.* 8:126(2019).
29. Ferro D,et,al.New Insights into the Pathogenesis of Non-Alcoholic Fatty Liver Disease: Gut-Derived Lipopolysaccharides and Oxidative Stress.*Nutrients.* 12:2762(2020).
30. Xiaofan J,Juan Z,Shixiu Z,Baozhen W,Chaodong W,Xin G.Advances in the Involvement of Gut Microbiota in Pathophysiology of NAFLD.*Front Med (Lausanne).* 7:361(2020).
31. Chen J,Vitetta L.Gut Microbiota Metabolites in NAFLD Pathogenesis and Therapeutic Implications.*Int J Mol Sci.* 21:5214(2020).

32. Egresi A,et,al.The potential role of organic and conventional yoghurt consumption in the treatment of non-alcoholic fatty liver disease.*Orv Hetil.* 61:1466-1474(2020).
33. Longlong L,Xu C,Yao Y,Ji C,Qian L,Haitian M.(-)-Hydroxycitric acid alleviates oleic acid induced steatosis, oxidative stress and inflammation in primary chicken hepatocytes by regulating AMPK mediated ROS levels.*J Agric Food Chem.* 68:11229-11241(2020).
34. Xiangjin X,Wenqing W,Lu L,Pin C.Liraglutide in combination with human umbilical cord mesenchymal stem cell could improve liver lesions by modulating TLR4/NF-kB inflammatory pathway and oxidative stress in T2DM/NAFLD rats.*Tissue Cell.* 66:101382(2020).
35. Yaxing Z,et,al.Si-Wu-Tang Alleviates Nonalcoholic Fatty Liver Disease via Blocking TLR4-JNK and Caspase-8-GSDMD Signaling Pathways.*Evid Based Complement Alternat Med.*8786424(2020).
36. Fenglian S,Zewei S,Shenghua J,Zhaozhong C.Erlotinib induces the human non-small-cell lung cancer cells apoptosis via activating ROS-dependent JNK pathways.*Cancer Med.* 5:3166-3175(2016).
37. Zhijie J,et,al.Oxidative stress, apoptosis and inflammatory responses involved in copper-induced pulmonary toxicity in mice.*Aging (Albany NY).* 12:16867-16886(2020).
38. Shujun Z,et,al.Propranolol induced apoptosis and autophagy via the ROS/JNK signaling pathway in Human Ovarian Cancer.*J Cancer.* 11:5900-5910(2020).
39. Kortam MA,Ali BM,Fathy N.The deleterious effect of stress-induced depression on rat liver: Protective role of resveratrol and dimethyl fumarate via inhibiting the MAPK/ERK/JNK pathway.*J Biochem Mol Toxicol.* :e22627(2020).
40. Ye-Kuan W,Lin-Feng H,De-Shuai L,Bo-Chu W,Jun T,Targeting DUSP16/TAK1 signaling alleviates hepatic dyslipidemia and inflammation in high fat diet (HFD)-challenged mice through suppressing JNK MAPK.*Biochem Biophys Res Commun.* 524:142-149(2020).

Tables

Table I.

Details of primary antibodies used in western blot analysis.

Name of first antibody	Origin	Manufacturer	Art. No	Dilution method	Dilution ratio
GAPDH	Rabbit	Abcam	ab37168	5% evaporated milk	1:10000
P-JNK	Rabbit	CST	#9251	5% BSA	1:1000
Caspase-3	Rabbit	Abcam	ab49822	5% evaporated milk	1:1000
Bax	Rabbit	CST	#2772	5% BSA	1:2000
ZO-1	Mouse	Santa	sc-33725	5% evaporated milk	1:500

GAPDH, glyceraldehyde-3-phosphate dehydrogenase; P-JNK, phosphorylation c-Jun N-terminal kinase; Caspase-3,cysteinyl aspartate specific proteinase-3; Bax,Bcl-2 Associated X Protein; ZO-1, Zonula occludens protein 1.

Table II.

Details of secondary antibodies used in Western blot analysis.

Name of secondary antibody	Manufacturer	Art. No	Dilution method	Dilution ratio
HRP-goat anti rabbit	ASPEN	AS1107	5% evaporated milk	1:10000
HRP-goat anti mouse	ASPEN	AS1106	5% evaporated milk	1:10000

Table III.

Sequences of mouse primers used for RT-qPCR.

Primer name	Primer sequence	Product length (bp)
M-GAPDH		227
sense	5'-TGAAGGGTGGAGCCAAAAG-3'	
antisense	5'-AGTCTTCTGGGTGGCAGTGAT-3'	
M-Bax		191
sense	5'-AGGATGCGTCCACCAAGAAG-3'	
antisense	5'-GTAGAAGAGGGCAACCACGC-3'	
M-Caspase3		189
sense	5'-GGAGAAATTCAAAGGACGGG-3'	
antisense	5'-GCATGGACACAATACACGGG-3'	
GAPDH, glyceraldehyde-3-phosphate dehydrogenase; Bax, Bcl-2 Associated X Protein; Caspase-3,cysteinyl aspartate specific proteinase-3 ;		

Table IV.

Details of the primary antibodies used for immunohistochemistry.

Name	Species	Manufacturer	Art. No	Dilution ratio
P-JNK	Rabbit	CST	#4668	1:50
Caspase3	Rabbit	CST	#9664	1:150
Bax	Rabbit	CST	#8663	1:150

Table V.

Details of the secondary antibodies used for immunohistochemistry.

Name	Manufacturer	Art. No	Dilution ratio
HRP-labeled rabbit anti-goat	Aspen	AS-1108	1:200
HRP-labeled goat anti-rabbit	Aspen	AS-1107	1:200
HRP-labeled goat anti-mouse	Aspen	AS-1106	1:200
HRP-labeled goat anti-rat	Aspen	AS-1093	1:200

Figures

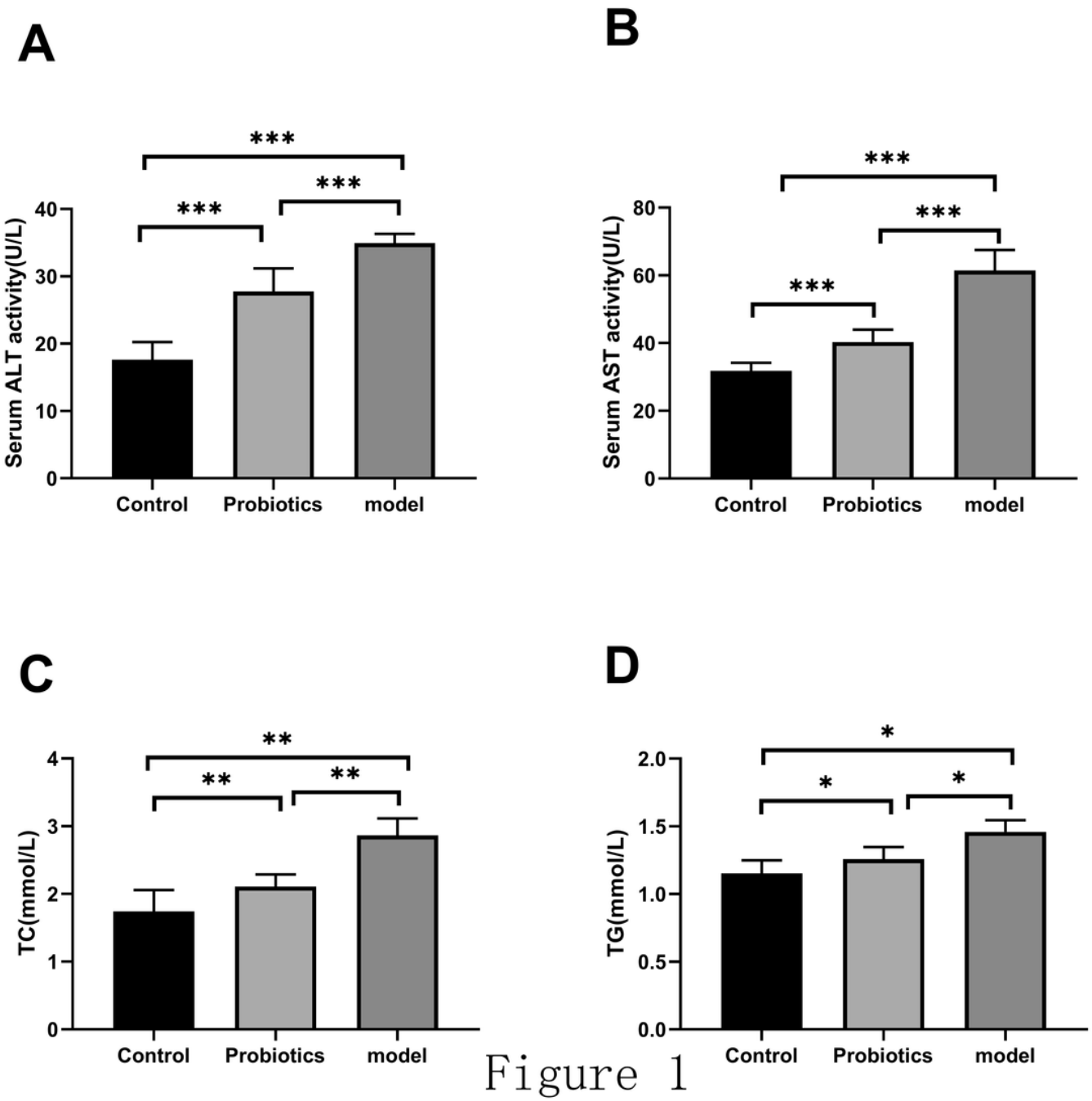

Figure 1

Figure 1

Serum AST, ALT, TC, and TG levels in each group. (A) Level of ALT. (B) Level of AST. (C) Level of TC. (D) Level of TG. *P < 0.05, **P < 0.01, ***P < 0.001. AST, aspartate aminotransferase; ALT, alanine aminotransferase; TG, triglyceride; TC, total cholesterol.

Figure 2

Hematoxylin and eosin staining of liver tissue from mouse in each group. Hematoxylin and eosin staining of liver tissue from mouse in: (a) the control group at magnification x 200 and (A) the control group at

magnification x 400; (b) the probiotic group at magnification x 200 and (B) probiotic group at magnification x 400; (c) the model group at magnification x 200 and (C) the model group at magnification x 400. The black arrows indicate steatosis, and the red arrows indicate inflammatory cell infiltration.

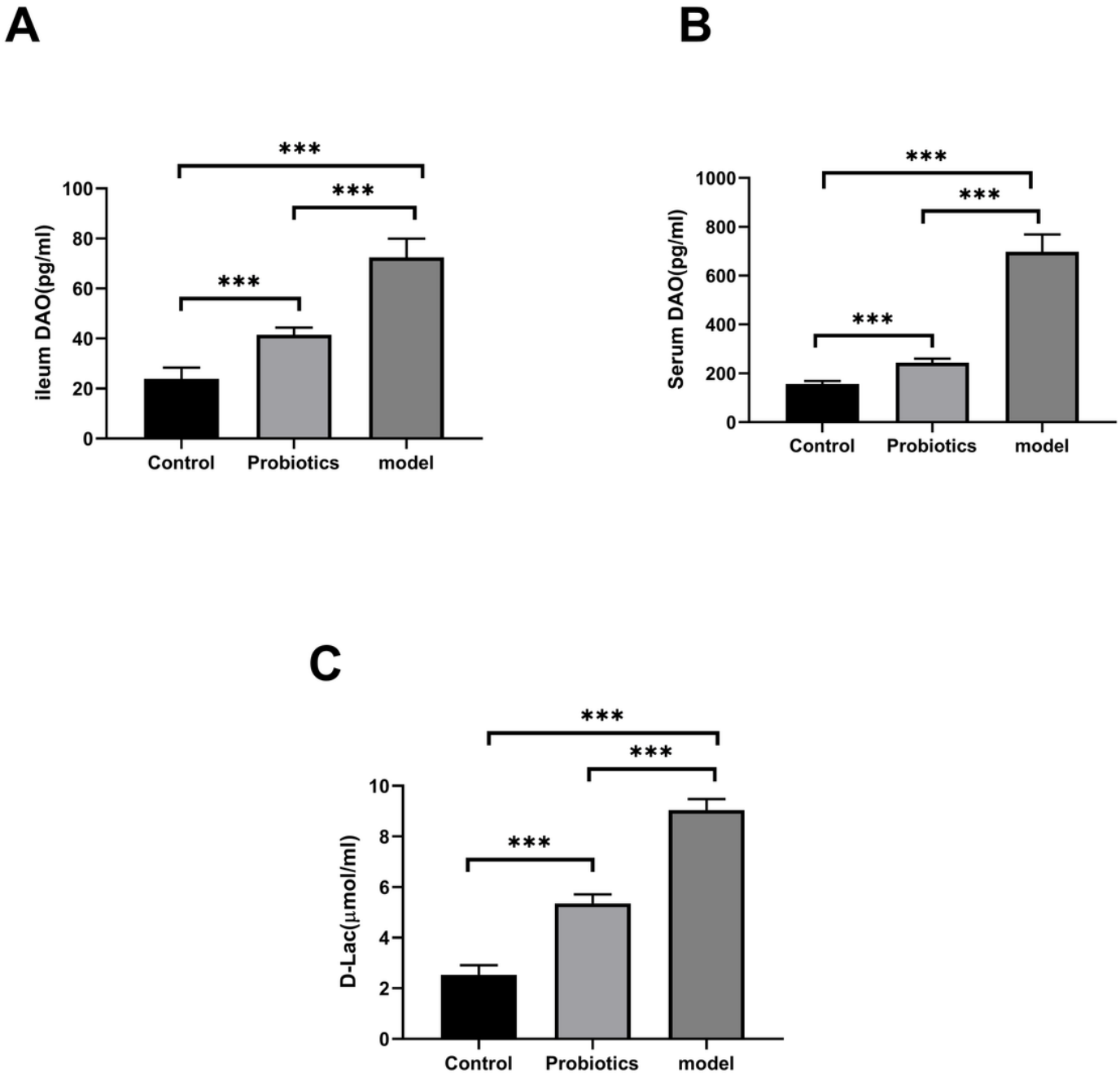

Figure 3

Serum D-Lac, DAO and ileum DAO levels in each group. (A) Ileum level of DAO. (B) Serum level of DAO. (C) Serum level of D-Lac.*P < 0.05, **P < 0.01, ***P < 0.001. DAO, diamine oxidase; D-Lac, D-lactic acid.

Figure 4

Hematoxylin and eosin staining of ileum tissue from mouse in each group. Hematoxylin and eosin staining of ileum tissue from mouse in: (a) the control group at magnification x 200 and (A) the control group at magnification x 400; (b) the probiotic group at magnification x 200 and (B) the probiotic group at magnification x 400; (c) the model group at magnification x 200 and (C) the model group at magnification x 400.

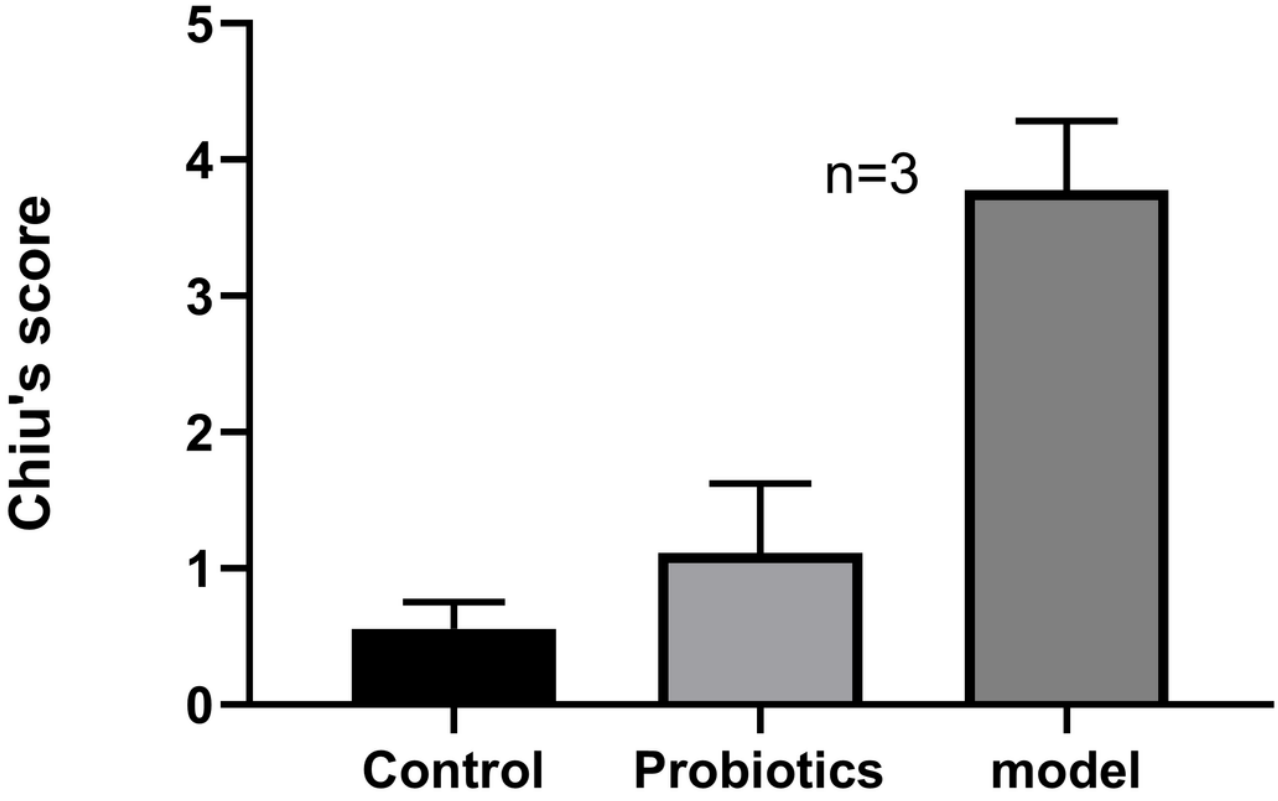

Figure 5

Chiu's score of the ileum tissue in each group.

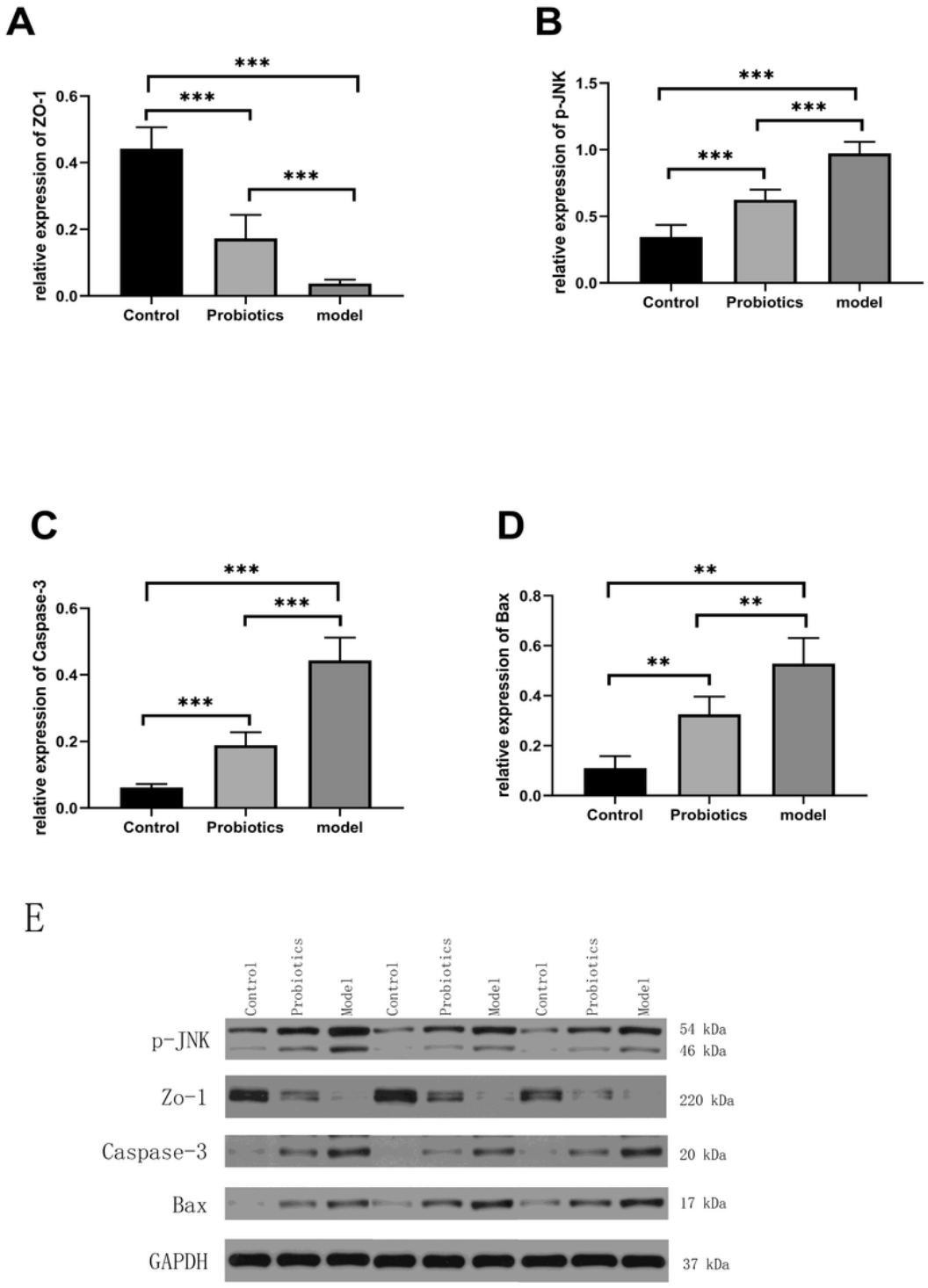

Figure 6

Western blot analysis was performed to compare the associated protein levels of JNK signaling pathway and intestinal barrier functional protein in each group. (A) Levels of ZO-1 protein. (B) Levels of p-JNK protein. (C) Levels of Caspase-3 protein. (D) Levels of Bax protein. (E) ZO-1 protein expression in the small intestine tissue of mice and the p-JNK, Caspase-3, and Bax protein expression in the liver tissue of

mice. *P < 0.05, **P < 0.01,***P < 0.001. ZO-1, zonula occludens protein 1; Caspase-3, cysteinyl aspartate specific proteinase-3; Bax, Bcl-2-associated X Protein; P-JNK, phosphorylation c-Jun N-terminal kinase.

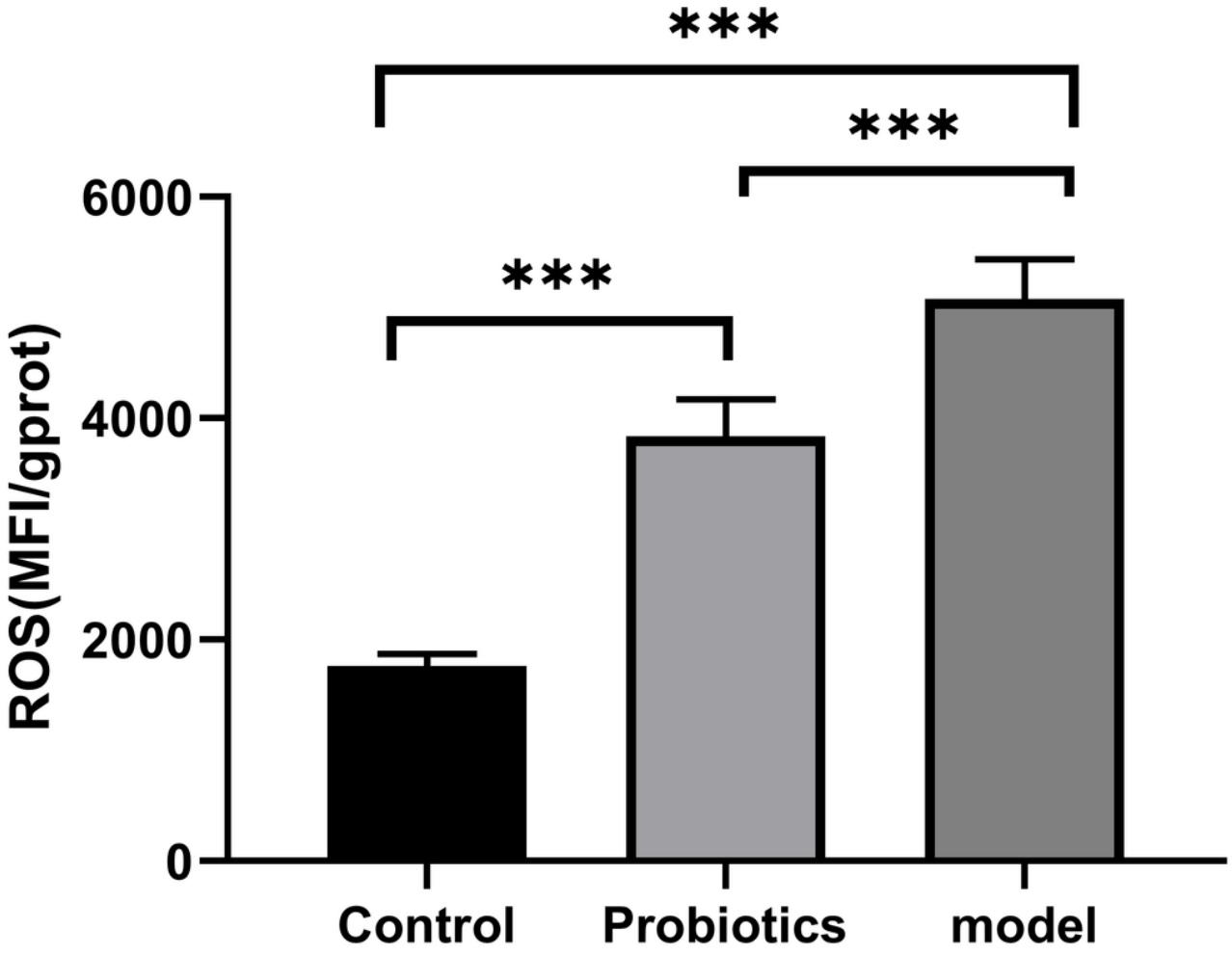

Figure 7

ROS levels in liver tissue in each group. *P < 0.05, **P < 0.01, P*** < 0.001. ROS, reactive oxygen species.

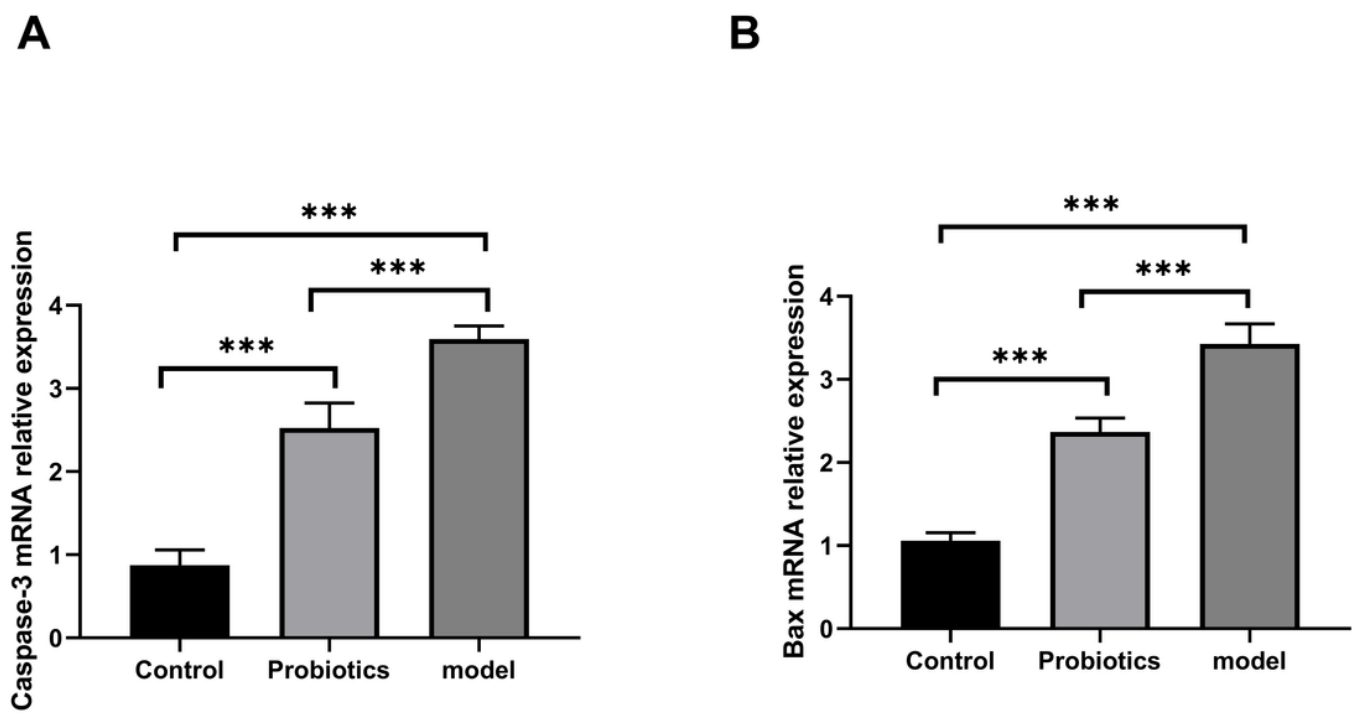

Figure 8

The mRNA levels of JNK signaling pathway. (A) The mRNA levels of Caspase-3. (B) The mRNA levels of Bax.*P < 0.05, **P < 0.01, P*** < 0.001.

Figure 9

Immunohistochemical levels for the JNK signaling pathway. The expression levels of (A) p-JNK, (B) Caspase-3, and (C) Bax were detected by immunohistochemical staining in the control, probiotics, and model groups.